福山大学　大学教育センター　大学教育論叢
第 4 号（2017 年度）　2018 年 3 月発行

Differential Interactions of LAMP-’s Lysosome-targeting Signals Containing Various COOH-terminal Amino Acid Residues with a Medium Subunit of Adaptor Protein Complex-2

Toshiyuki HATA, Hiroshi SAKANE, Misato UEDA,

Misa MIYOSHI, Junzo HIROSE, Kenji AKASAKI

Differential Interactions of LAMP-1's Lysosome-targeting Signals Containing Various COOH-terminal Amino Acid Residues with a Medium Subunit of Adaptor Protein Complex-2

Toshiyuki HATA* Hiroshi SAKANE** Misato UEDA*** Misa MIYOSHI***
Junzo HIROSE* Kenji AKASAKI*

種々のC末端アミノ酸残基を有するリソソーム膜タンパク質1輸送シグナルとアダプタータンパク質2の中サブユニットとの異なる相互作用

秦 季之* 坂根 洋** 上田美里*** 三好未紗*** 廣瀬順造* 赤﨑健司*

ABSTRACT

Lysosome-associated membrane protein-1 (LAMP-1) is a type I membrane glycoprotein with a COOH-terminal lysosome-targeting signal peptide of $G^{1}YQTI^{5}$-COOH. This sequence is categorized as a tyrosine-based motif of GYXXΦ where Φ is a bulky hydrophobic amino acid residue. Lysosomal localization of LAMP-1 varies by changing the Φ amino acid residues. In this study, we conducted computer-based molecular modeling for structures of the COOH-terminal wild-type and mutant peptides (GYQTI, GYQTL, GYQTF, GYQTM, and GYQTV) complexed with a medium subunit of adaptor protein complex-2 (μ2 of AP-2), a key molecule in vesicular transport to endosomes and lysosomes. Tyr2 of all the peptides is critical for their rigid binding to μ2 by well fitted hydrogen bonds and hydrophobic interactions between Tyr2 and the surrounding amino acids of μ2. The Φ hydrophobic side chains of LAMP-1-derived COOH-terminal peptides are located exclusively within a hydrophobic pocket formed by five hydrophobic amino acid moieties on β-sheets of μ2, whereas slight but significant differences were observed in the spatial position of the side chain of a Φ residue in the hydrophobic pocket, causing their differential affinities with μ2. These results could explain, at least in part, why the COOH-terminal variants of LAMP-1 show different lysosomal localization in late endosomes and lysosomes.

Keywords: molecular modeling, adaptor protein complex-2, μ2 subunit, tyrosine-based motif, binding affinity

1. Introduction

Lysosomes are membrane-limited intracellular organelles involved in endocytic and autophagic processes and possess an assortment of soluble acid-dependent hydrolases and a set of integral membrane glycoproteins.[1-4] LAMP-1 and LAMP-2 are structurally similar to each other and account for a major portion of lysosomal membrane proteins.[5-9] Both of the LAMPs consist of a large and highly glycosylated luminal domain, a single transmembrane domain and a short cytoplasmic tail at the COOH-terminal. Targeting of LAMP-1 and LAMP-2 to lysosomes is dependent upon a tyrosine-based motif of the COOH-terminal cytoplasmic tail, which conforms to GYXXΦ.[10-14] Although it was previously assumed that Φ would be any bulky hydrophobic amino acid residue for lysosomal localization, studies in the last two decades[13,14] have shown that the lysosomal localization of LAMP-1 and LAMP-2 varies by changing hydrophobic amino acid residues in the Φ position and that COOH-terminal isoleucine occurring in wild-type (WT) LAMP-1 is optimal for its efficient targeting to dense lysosomes. The tyrosine-based motif is reportedly bound to a medium chain of adaptor protein complex-2 (μ2 of AP-2), a key molecule in the vesicular transport of intrinsic lysosomal and internalized proteins to their final destinations.[15-20] Deletion of μ2 from cells caused a significant decrease in the amounts of newly synthesized LAMP-1 transported to lysosomes.[21] In consideration of all these findings, therefore, it is important to determine the ternary structures of its various COOH-terminal amino acid-containing tyrosine-based peptides complexed with μ2 in order to elucidate the exact role played by AP-2 in the lysosomal transport of LAMP-1

*大学教育センター共通教育担当教員・薬学部教授 **薬学部講師 ***薬学部

Notable successes have been achieved by computational methods that model the structures of proteins with sufficient accuracy to facilitate functional studies. [22] Because the crystal structure of the tyrosine-based signal binding domain of μ2 was solved (Fig. 1),[17] we herein conducted molecular modeling for LAMP-1's intrinsic signal peptide and its COOH-terminal variants associated with μ2 and found that these peptides have differential interactions with μ2, providing a possible explanation for the COOH-terminus-dependent transportation of LAMP-1 to lysosomes.

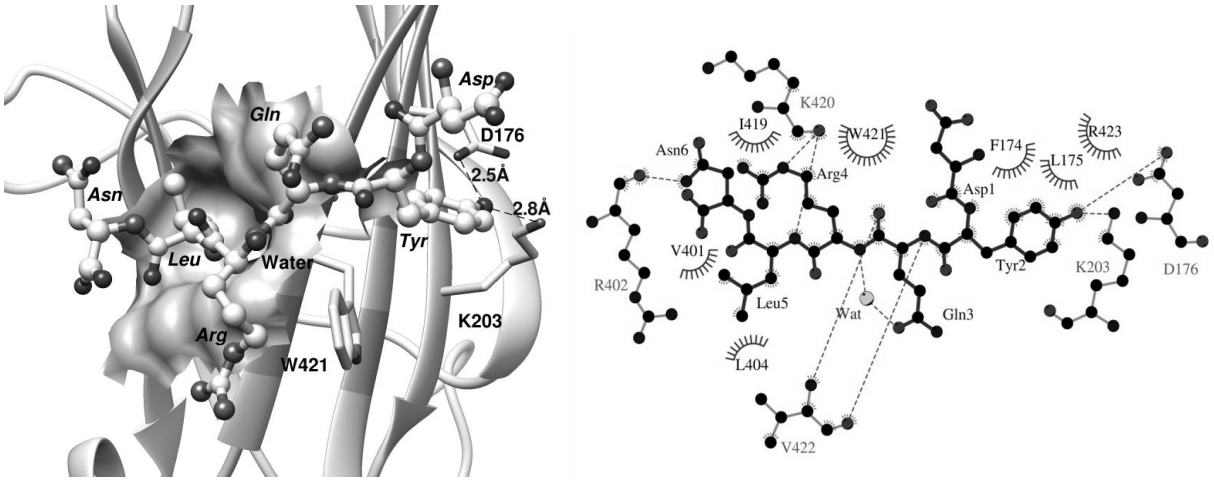

a) Structure b) Interaction diagram

Figure 1. X-ray crystal structure of the complex formed between TGN38 (DYQRLN) and the μ2 subunit of AP-2 and the interaction diagram of the TGN38 peptide with the μ2 subunit of AP-2.

μ2 subunit and TGN38 were shown as a stick and ball and stick model, respectively. The hydrogen bonds were indicated by dashed lines. The interaction diagram was drawn by LIGPLOT. The hydrogen bonds were indicated by dashed lines between the atoms involved, and the hydrophobic contacts were represented by an arc with spokes radiating toward the ligand atoms they contact.

2. Materials and Methods

(1) Homology modeling of the complexes between the GYQTΦ peptides and μ2.

The molecular modeling was performed by a SWISS-MODEL homology modeling server[23] using a rat μ2 structure (PDB ID: 1BXX)[17] as a template. The X-ray crystal structure of the 1BXX unfortunately lacked the protein conformation from Val221 to Gly237 in the rat μ2. The amino acid sequence of μ2 necessary for homology modeling was obtained from the UniProt database (ID: P84092 - AP2M1_RAT). [24] The range of residues that the SWISS-MODEL server[23] generated was Ile156 to Cys435. The protonation states of these three-dimensional models were assigned by the PDB2PQR server.[25,26] In Fig. 1, one water molecule forms two hydrogen bonds to an oxygen atom of the side chain of the Gln3, and to a nitrogen atom of the main chain of the Arg4. Since it is assumed that this water molecule is important to pack the TGN38 -derived peptide (DYQRLN) with Trp421, the water molecule hydrogen bonding to the GYQTΦ peptide is taken into account in the molecular modeling. The geometries of GYQTΦ (Φ= F, I, L, M and V) peptides with one water were modified on the basis of that of DYQRLN included in the crystal structure (PDB ID: 1BXX).[17]

(2) Energy minimization for the complex between the GYQTΦ peptides with one water molecule and μ2

The energy minimizations of the complex between the GYQTΦ peptide and μ2 were carried out using the AMBER12 suite[27] with the parm03 force field and a solvation effect by the generalized Born/surface area (GB/SA) method. All calculations were employed on an NEC Parallel Cluster System at the Research Center for Green Science, Fukuyama University.

(3) Prediction of the binding constant between the GYQTΦ peptides and μ2

The binding constant was predicted by using Autodock Vina[28] software with the local search method. A docking grid with a size of 30Å x 30Å x 30Å was used. The center of the docking grid was the CG atom of Asp18 of μ2 obtained by the energy minimization. The Autodock Vina presents the docking scores as the free energy of binding (ΔG_b). The predicted binding constant (K_b) for all docking runs was calculated from the ΔG_b value as follows: $K_b=\exp((-\Delta G_b \times 1{,}000)/RT))$, where R is 1.9872 cal·K^{-1}·mol^{-1} and T is 300 K.

3. Results

(1) Molecular modeling of the complexes between the GYQTΦ peptides and μ2

The molecular modeling of the complexes between GYQTΦ peptides and μ2 was performed with a SWISS-MODEL homology modeling server using the rat μ2 subunit of the AP-2 structure (PDB ID: 1BXX)[17] as a template. The geometries of the GYQTΦ (Φ=F, I, L, M, and V) peptides were produced on the basis of those of the TGN38-derived peptide (DYQRLN) included in the μ2 crystal structure (PDB ID: 1BXX), as shown in Fig. 1. All energy minimizations of the complex structures between GYQTΦ peptides and μ2 were carried out as described in the Materials and Methods. The models of the complex structures between GYQTΦ peptides and μ2 are shown in Fig. 2.[29] Two-dimensional schematic representations[30] of the interactions between GYQTΦ peptides and μ2 are provided in Fig. 3.

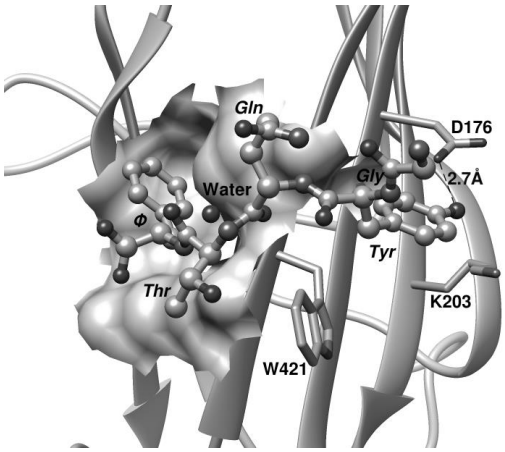

GYQTF

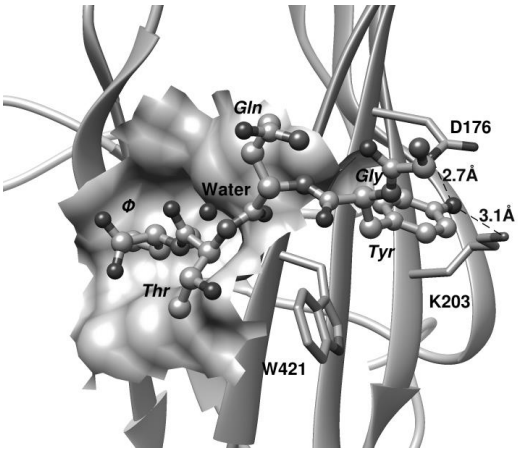

GYQTI

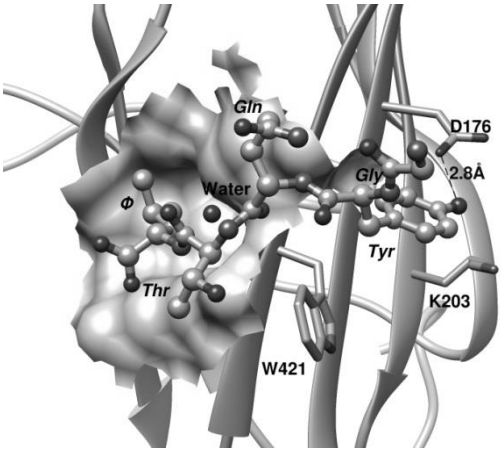

GYQTL

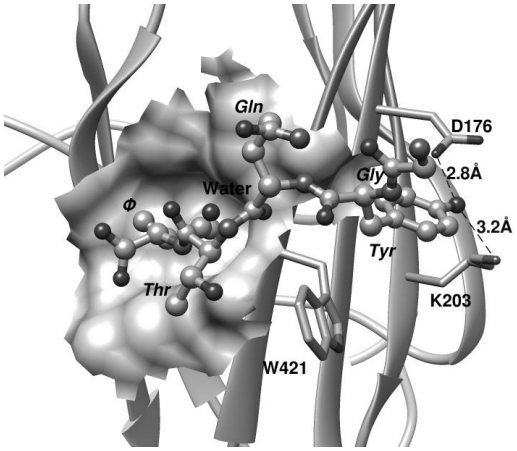

GYQTV

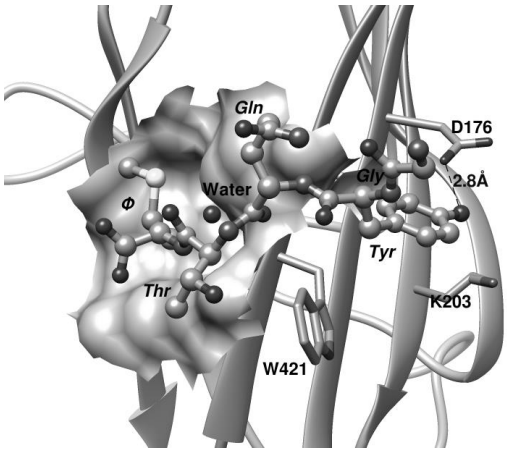

GYQTM

Figure 2. Structures of GYQTΦ peptide docking with the μ2 subunit of AP-2.
The μ2 subunit and GYQTΦ peptide were shown as a stick and ball and stick model, respectively. The hydrogen bonds were indicated by dashed lines.

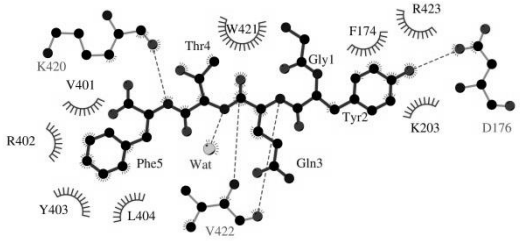

GYQTF

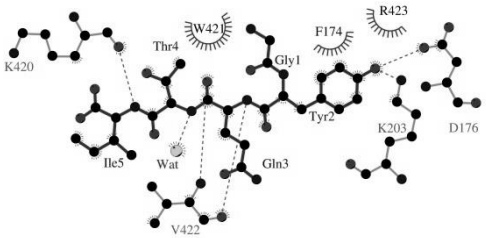

GYQTI

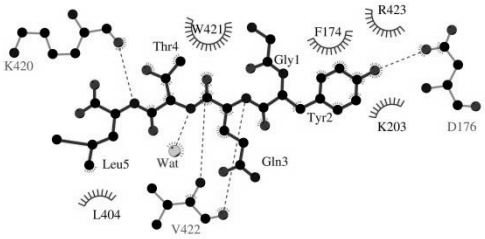

GYQTL

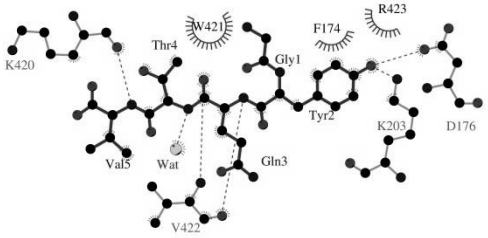

GYQTV

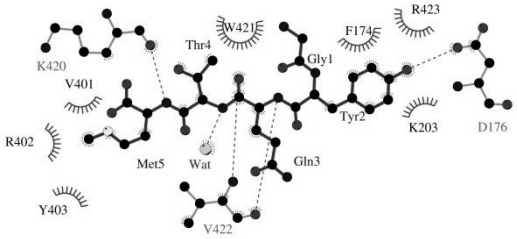

GYQTM

Figure 3. Interactions diagrams between GYQTΦ and the μ2 subunit.
All figures are drawn by LIGPLOT. The hydrogen bonds were indicated by dashed lines between the atoms involved, and the hydrophobic contacts were represented by an arc with spokes radiating toward the ligand atoms they contact.

All three-dimensional (3D) structures of the complexes between GYQTΦ peptides and μ2 closely resembled each other, and also closely resembled the 3D structures of the complexes between the TGN38-peptide

and μ2. Hydrophobic interactions were observed between the tyrosine ring and Phe174 and Arg423 of μ2 in all the complexes. The phenolic hydroxyl group of Tyr2 forms a hydrogen bond with the carboxylate of Asp176. Moreover, Tyr2 of the GYQTI and GYQTV peptides makes another side chain hydrogen bond to an εN of Lys203 of μ2. These hydrophobic interactions and hydrogen bonds around Tyr2 cause the rigid binding of GYQTΦ to μ2. In addition, the side chain of the Φ amino acid contributes to the binding of LAMP-1-derived peptides to μ2. The side chain of the Φ amino acid was located in the hydrophobic pocket formed by Leu173, Leu175, Val401, Leu404, and Val422 residues on β-sheets of μ2, and the chain came into contact with Val401, Tyr403, Leu404, and the aliphatic portion of Arg402.

We next superimposed only GYQTΦ peptides selected from their complexes with μ2 (Fig. 4). The main chains of the five GYQTΦ peptides overlapped very well, whereas the side chains were rotated relative to the α-carbon of Φ depending on the amino acid residues.

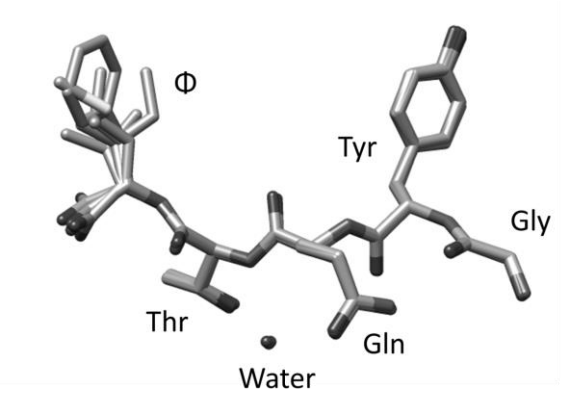

Figure 4. Superimposition of GYQTΦ peptides docking with the μ2 subunit of AP-2.

(2) Binding affinity (ΔG_b), binding constants (K_b), and buried surface areas between GYQTΦ peptides and μ2

The binding affinity (ΔG_b) and binding constants (K_b) of the complex between GYQTΦ peptides and μ2 were computationally determined and are shown in Table 1.

Table 1. Binding affinities (ΔG_b), binding constants (K_b) and buried solvent-excluded surface areas between GYQTΦ peptides and the μ2 subunit of AP-2

GYQTΦ peptide	Binding Affinity ΔG_b [a)]	Binding constants K_b [b)] at 300 K	Buried solvent-excluded surface area [c)]	Relative abundances (percentage of the total) of LAMP-1 and the mutants in late endosomes and lysosomes [d)]		Interactions between LAMP-2b mutants and μ2 subunit of AP-2 detected by the yeast two hybrid system [e)]	
	(kcal/mol)	(L/mol)	(Å)	CT-Sequence	%	CT-Sequence	Interaction
GYQTF	−5.56	11,150	194	GYQTF	4.5	GYQSF	++
GYQTI	−5.32	7,575	197	GYQTI	19	GYQSI	+
GYQTL	−5.13	5,461	184	GYQTL	11	GYQSL	++
GYQTV	−4.94	3,971	166	GYQTV	3.0	GYQSV	—
GYQTM	−4.55	2,080	142	GYQTM	4.2	GYQSM	—

a) The binding affinity (ΔG_b) was obtained using the Autodock Vina program.

b) Binding: $E + L = EL$; $K_b = [EL]/[E][L]$; $\Delta G_b = -RT \ln K_b$; $K_b = \exp(-\Delta G_b /RT)$.

c) The values were obtained by the "measure buried" command in the UCSF Chimera program.

d) Akasaki K., Suenobu M., Mukaida M., Michihara A., Wada I. (2010) *J. Biochem.*, Vol. 148, No. 6, 669-679.

e) Gough N. R., Zweifel M. E., Martinez-Augustin O., Aguilar R. C., Bonifacino J. S., Fambrough D. M. (1999) *J. Cell. Sci.*, Vol. 112, No. 23, 4257-4269. The strengths of the interaction are indicated by the number of (+) symbols. A (−) symbol indicates the absence of any interaction.

The ΔG_b values for GYQTF, GYQTI, GYQTL, GYQTM, and GYQTV were -5.56, -5.32, -5.13, -4.94, and -4.55 kcal/mol, respectively. The K_b values derived from the ΔG_b for GYQTF, GYQTI, GYQTL, GYQTM, and GYQTV were 11,150, 7575, 5461, 3971, and 2180, respectively. The order of the binding affinities of the complex GYQTΦ (Φ=F, I, L, M and V) peptides and the μ2 subunit of AP-2 was Φ=F >> I > L > M >> V. These binding affinities were in good agreement with those obtained from the yeast-two hybrid method, but their order was not necessarily coincident with the relative abundance of the WT and the COOH-terminal mutants of LAMP-1 in late endosomes and lysosomes.[14] It was noteworthy that LAMP-1 containing GYQTI and GYQTL with moderate affinities for μ2 was localized at the highest levels in late endosomes and lysosomes (Table 1). These results suggested that the highest affinity GYQTF hampered dissociation from μ2 after the GYQTF-LAMP-1 mutant was included in transport vesicles, resulting in the lower rate of delivery of this mutant to late endosomes and lysosomes. The buried solvent-excluded surface (BSES) areas[26] for GYQTF, GYQTI, GYQTL, GYQTM, and GYQTV were 194, 197, 184, 166, and 142 Å^2, respectively. The relationship between the binding affinity (ΔG_b) and the buried solvent-excluded surface areas is shown in Fig. 5.

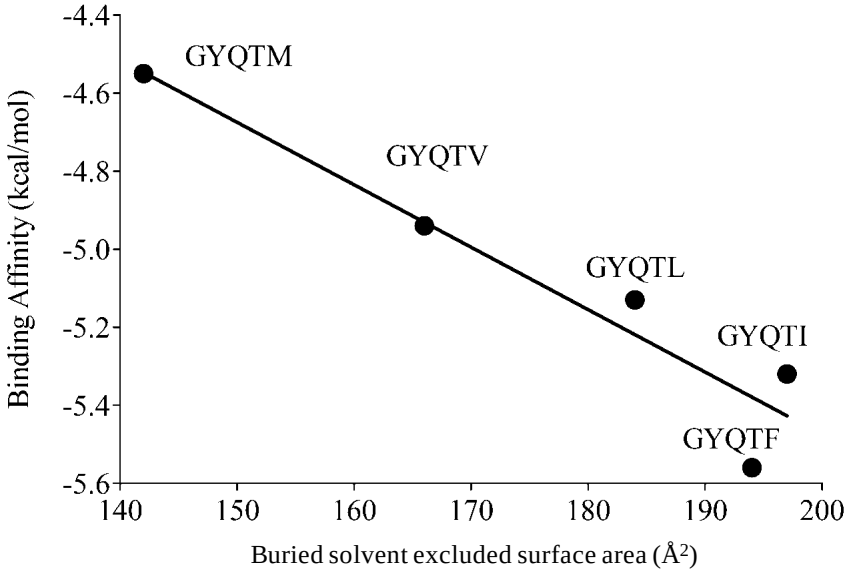

Figure 5. Relationship between the binding affinities and buried solvent-excluded surface areas.
The linear regressions for the binding affinity (ΔG_b) and the buried solvent-excluded surface (BSES) areas were represented by the following equation. $\Delta G_b = -0.016 \times (BSES) - 2.275$, $r^2 = 0.912$.

The binding affinities increased with the increase in the BSES areas. The linear regressions for the binding affinity (ΔG_b) and the BSES areas are represented by the following equations.

$$\Delta G_b = -0.016 \times (BSES) - 2.275, \quad r^2 = 0.912.$$

The square of the correlation between the binding affinity and the buried solvent-excluded surface area was 0.912. These results indicated that the differential affinities of GYQTΦ with μ2 were closely related to the different interactions of the Φ side chains with the side chains of the amino acid residues that constitute the pocket.

4. Discussion

X-ray crystal structure analysis of the complex between the TGN38 peptide (DYQRLN) and μ2 of AP-2 showed that the hydroxyl group of Tyr2 formed a hydrogen bond with the oxygen atom of the Asp176 of μ2, and the side chain of the Φ residue (Leu5) of the TGN38 peptide was located in the hydrophobic pocket formed by Leu173, Leu175, Val401, Leu404, and Val422, as shown in Fig. 1. In this paper, the structures of the complex formed between the GYQTΦ (Φ=F, I, L, M and V) peptides and μ2 were predicted by molecular modeling. These predicted structures were very similar to those of the complex between the TGN38 peptide and μ2. Significant differences were observed in the 3D structure among the GYQTΦ (Φ=F, I, L, M and V) peptides; the side chains of Φ make subtle but significant differences at a position relative to the α-carbon of Φ.

As shown in Table 1, the predicted binding affinities between the complex GYQTΦ (Φ=F, I, L, M, V) peptides and the μ2 subunit of AP-2 were Φ=F >> I > L > M >> V. The *in vivo* binding strength of μ2 to GYQTΦ

is generally assessed by a binding constant (K_b) calculated from a binding affinity (ΔG_b). The K_b value of μ2 subunit for GYQTI is 1.9 and 3.6 times higher than those for GYQTM and GYQTV, respectively, and 1.5 times lower that for GYQTF (Table 1, column 3). These differences could affect the efficient transport of LAMP-1 to late endosomes and lysosomes (Table 1, column 6). It is currently unknown whether the subtle difference in affinities between μ2 and GYQTΦ peptides has biological significance in cellular function. The optimal affinity of the LAMP-1's tail with μ2 is seemingly present in the efficient transport of LAMP-1 to the lysosome to maintain an appropriate amount of LAMP-1 for the lysosomal function. The yeast two-hybrid assays distinguished the subtle difference in interactions between LAMP-1/LAMP-2b chimera targeting signals (GYQSΦ). The μ2 subunit of the AP-2 adaptor and their strengths were F(++), I(+), L(++), V(–), and M(–), respectively.[13] The trends observed for the interaction between the GYQTΦ residue and μ2 were very similar to those for the interaction between the GYQSΦ residue and μ2. These results can be explained by the loss of the hydrophobic stacking interaction. Moreover, the binding affinity was correlated to the buried surface of the complex GYQTΦ peptides and μ2. It is known that the buried surface of the complex is related to the binding affinity.[31] As mentioned above, since the difference of the 3D structure in GYQTΦ arises only from the Φ side chain of GYQTΦ peptides, the difference in the buried surface of the complex formed between GYQTΦ peptides and μ2 can be attributed to the difference in the surface area of the side chain of Φ. It is clear that the van der Waals interaction between the side chain of the Φ residue in the GYQTΦ peptides and the μ2 subunit of AP-2 plays an important role in the binding affinity.

5. Conflict of Interest

The authors declare no conflict of interest.

References

1) Holtzman E.(1989) *Lysosome.* Plenum Press, New York.
2) Kornfeld S., Mellman I. (1989) "The biogenesis of lysosomes." *Annu. Rev. Cell. Biol.,* Vol. 5, 483-525.
3) Luzio J. P., Pryor P. R., Bright N. A. (2007) "Lysosomes: fusion and function." *Nat. Rev. Mol. Cell Biol.,* Vol. 8, No. 8, 622-632.
4) Braulke T., Bonifacino J. S. (2009) "Sorting of lysosomal proteins." *Biochim. Biophys. Acta*., Vol. 1793, No. 4, 605-614.
5) Chen J. W., Cha Y., Yuksel K. U., Gracy R. W., August J. T. (1988) "Isolation and sequencing of a cDNA clone encoding lysosomal membrane glycoprotein mouse LAMP-1. Sequence similarity to proteins bearing onco-differentiation antigens." *J. Biol. Chem.,* Vol. 263, No. 2, 8754-8758.
6) Cha Y., Holland S. M, August J. T. (1990) "The cDNA sequence of mouse LAMP-2. Evidence for two classes of lysosomal membrane glycoproteins." *J. Biol. Chem*., Vol. 265, No. 9, 5008-5013.
7) Fukuda M. (1991) "Lysosomal membrane glycoproteins. Structure, biosynthesis, and intracellular trafficking." *J. Biol. Chem*., Vol. 266, No. 32, 21327-21330.
8) Hunziker W., Geuze H. J. (1996) "Intracellular trafficking of lysosomal membrane proteins." *Bioessays,* Vol. 18, No. 5, 379-389.
9) Eskelinen S. A., Tanaka Y., Saftig P. (2003) "At the acidic edge: emerging functions for lysosomal membrane proteins." *Trends Cell Biol.,* Vol. 13, No. 3, 137-145.
10) Williams M. A., Fukuda M. (1990) "Accumulation of membrane glycoproteins in lysosomes requires a tyrosine residue at a particular position in the cytoplasmic tail." *J. Cell Biol*., Vol. 111, No. 3, 955-966.
11) Guarnieri F. G., Arterburn L. M., Penno M. B., Cha Y., August J. T. (1993) "The motif Tyr-X-X-hydrophobic residue mediates lysosomal membrane targeting of lysosome-associated membrane protein 1." *J. Biol. Chem*., Vol. 268, No. 3, 1941-1946.
12) Höning S., Hunziker W. (1995) "Cytoplasmic determinants involved in direct lysosomal sorting, endocytosis, and basolateral targeting of rat lgp120 (lamp-I) in MDCK cells." *J. Cell Biol.,* Vol. 128, No. 3, 321-332.
13) Gough N. R, Zweifel M. E., Martinez-Augustin O., Aguilar R. C., Bonifacino J. S., Fambrough D. M.

(1999) “Utilization of the indirect lysosome targeting pathway by lysosome-associated membrane proteins (LAMPs) is influenced largely by the C-terminal residue of their GYXXΦ targeting signals.” *J. Cell Sci.*, Vol. 112, No. 23, 4257-4269.

14) Akasaki K., Suenobu M., Mukaida M., Michihara A., Wada I. (2010) “COOH-Terminal Isoleucine of Lysosome-Associated Membrane Protein-1 (LAMP-1) Is Optimal for Its Efficient Targeting to Dense Secondary Lysosomes.” *J. Biochem.*, Vol. 148, No. 6, 669-679.
15) Ohno H., Aguilar R. C., Yeh D., Taura D., Saito T., Bonifacino J. S. (1998) “The Medium Subunits of Adaptor Complexes Recognize Distinct but Overlapping Sets of Tyrosine-based Sorting Signals.” *J. Biol. Chem.*, Vol. 273, No. 40, 25915-25921.
16) Stephens D. J. Banting G. (1998) “Specificity of interaction between adaptor-complex medium chains and the tyrosine-based sorting motifs of TGN38 and lgp120.” *Biochem. J.*, Vol. 335, No. 3, 567-572.
17) Owen D. J., Evans P. R. (1998) “A structural explanation for the recognition of tyrosine-based endocytotic signals.” *Science*, Vol. 282, No. 5329, 1327-1332.
18) Bonifacino J. S., Dell’Angelica E. C. (1999) “Molecular bases for the recognition of tyrosine-based sorting signals.” *J. Cell Biol.*, Vol. 145, No. 5, 923-926.
19) Owen D. J., Collins B. M., Evans P. R. (2004) “Adaptors for clathrin coats: structure and function.” *Annu. Rev. Cell Dev. Biol.*, Vol. 20, 153-191.
20) Robinson M. S. (2004) “Adaptable adaptors for coated vesicles.” *Trends Cell Biol.*, Vol. 14, No. 4, 167-174.
21) Janvier K. Bonifacino J. S. (2005) “Role of the Endocytic Machinery in the Sorting of Lysosome-associated Membrane Proteins.” *Mol. Biol. Cell.*, Vol. 16, No. 9, 4231-4242.
22) Hata T., Shibata Y., Okano M., Kodera A., Ueda M., Iwamoto H., Tomida H., Iwamoto H., Hirose J. (2015) “Flexibility of the Coordination Geometry at the N-Site of $Cu(II)_2$ Human Serum-Transferrin Induced by the Different Orientations of Arg124.” *Biol. Chem. Bull.*, Vol. 38, No. 3, 358-364.
23) Arnold K., Bordoli L., Kopp J., Schwede T. (2006) “The SWISS-MODEL workspace: a web-based environment for protein structure homology modelling.” *Bioinformatics*, Vol. 22, No. 2,195-201.
24) The UniProt Consortium (2015) “UniProt: a hub for protein information.” *Nucleic Acids Res*. Vol. 43, No. D1, D204-D212.
25) Dolinsky T. J., Nielsen J. E., McCammon J. A. (2004) “PDB2PQR: an automated pipeline for the setup of Poisson-Boltzmann electrostatics calculations.” Baker N. A., *Nucleic Acids Res*, Vol. 32, (Web Server Issue), W665-W667.
26) Dolinsky, T. J., Czodrowski, P., Li H., Nielsen J. E., Jensen J. H., Klebe G., Baker N. A. (2007) “PDB2PQR: expanding and upgrading automated preparation of biomolecular structures for molecular simulations.” *Nucleic Acids Res*, Vol. 35, (Web Server Issue), W522-525.
27) Case D. A., Darden T. A., Cheatham III T. E., Simmerling C. L., Wang J., Duke R. E., Luo R., Walker R. C., Zhang W., Merz K. M., Roberts B., Hayik S., Roitberg A., Seabra G., Swails J., Götz A. W., Kolossváry I., Wong K. F., Paesani F., Vanicek J., Wolf R. M., Liu J., Wu X., Brozell S. R., Steinbrecher T., Gohlke H., Cai Q., Ye X., Wang J., Hsieh M.-J., Cui G., Roe D. R., Mathews D. H., Seetin M. G., Salomon-Ferrer R., Sagui C., Babin V., Luchko T., Gusarov S., Kovalenko A., Kollman P. A., (2012), AMBER 12, University of California, San Francisco.
28) Trott O., Olson A. J. (2010) “AutoDock Vina: improving the speed and accuracy of docking with a new scoring function, efficient optimization, and multithreading.” *J. Comput. Chem.*, Vol. 31, No. 2, 455-461.
29) Pettersen E. F., Goddard T. D., Huang C.C., Couch G. S., Greenblatt D. M., Meng E. C., Ferrin T. E. (2004) “UCSF Chimera--a visualization system for exploratory research and analysis.” *J. Comput. Chem.*,

Vol. 25, No. 13, 1605-1612.

30) Laskowski R. A., Swindells M. B. (2011) "LigPlot+: multiple ligand-protein interaction diagrams for drug discovery." *J. Chem. Inf. Model.*, Vol. 51, No. 10, 2778-2786.

31) Chen J., Sawyer N., Regan L. (2013) "Protein–protein interactions: General trends in the relationship between binding affinity and interfacial buried surface area." *Protein Sci*., Vol. 22, No. 4, 510-515.